Archives of Mechanics • Archiwum Mechaniki Stosowanej • 29, 1, pp. 69–80, Warszawa 1977

Wave structure and density distribution in a nonstationary gas jet

I. M. NABOKO, V. V. GOLUB, A. V. EREMIN, V. A. KOCHNEV, A. A. KULIKOVSKY (MOSCOW)

THE PAPER deals with the unsteady jet flow when the ratio of the nozzle exit stagnation pressure to the ambient pressure varies in a wide range. A specific wave pattern during the initial stages of the supersonic outflow has been observed. The observed wave pattern is found to depend on the physical properties of the particular gas. Consideration is also given to time dependence of the flow structure and the density distribution in the unsteady jet. The generalized data for the gas front along the flow are found to be in fair agreement with calculation by a spherical source model. The time taken for the steady jet to be established as observed in the experiment is found to be an order of magnitude longer than that obtained by calculations.

Praca dotyczy nieustalonego wypływu strumienia w przypadku, gdy stosunek ciśnienia stagnacji wylotu dyszy do ciśnienia otaczającego waha się w szerokich granicach. Zaobserwowano specyficzny układ fal w początkowych stadiach wypływu naddźwiękowego, zależny od fizycznych własności zastosowanego gazu. Rozważono również zmienność czasową struktury przepływu i rozkładu gęstości w nieustalonym strumieniu. Stwierdzono dobrą zgodność danych dotyczących przebiegu frontu fali wzdłuż strumienia z obliczeniami wynikającymi z przyjęcia modelu sferycznego. Czas potrzebny do ustalenia się przepływu mierzony doświadczalnie okazuje się o jeden rząd wielkości większy od otrzymanego na drodze obliczeniowej.

Работа касается неустановившегося истечения потока в случае, когда отношение критического давления выхода сопла к окружающему давлению изменяется в широких пределах. Наблюдается специфическая система волн в начальных стадиях сверхзвукового истечения, зависящего от физических свойств применяемого газа. Рассмотрено тоже изменение во времени структуры течения и распределения плотности в неустановившемся потоке. Констатировано лишь приемлемое согласе данных, касающихся хода фронта волны вдоль потока, с расчетами следующими из принятия сферической модели. Время необ ходимое для установления течения, измеренное экспериментально, оказывается на один порядок величины больше, чем время полученное путем расчета.

THE FIRST experimental observation for a long period of time of a nonstationary outflowing jet was made by the authors of [1]. The results of this work showed the failure of the ideal theory calculation to determine the time required for a stationary flow to develop [2], and indicated the need for a more detailed analysis of nonstationary stage, essential in many applied and fundamental problems such as pulse gas-dynamic lasers, rocket engines, evaporation of a substance from a solid surface by pulse laser radiation.

Several theoretical studies are at present available, which describe the nonstationary jet from a source in terms of different models. Paper [3] studies an asymptotic behaviour of a primary or external shock wave, the contact surface, a secondary shock wave at the final stage of the process for the ideal gas. The behaviour of the secondary shock has been noted to depend on the ratio of the jet stagnation temperature to the temperature

of the ambient gas. The nonstationary outflow of viscous heat-carrying gas is considered in paper [4]. The author has found an approximate equation of motion of the jet front and has made numerical calculation of the flow parameters in terms of the Navier-Stokes equation.

The formation of a stationary flow on the jet and in the nozzle proceedes through two stages: a stage during which all the disturbances associated with the jet front pass by a given point, and a stage of development of a steady-state flow.

The establishment of stationary parameters upstream the secondary shock wave does not depend on the counter-pressure. The time required for the flow to become stationary is a function of the type of the flow symmetry and physical and chemical parameters of the gas.

The present investigation deals with nonstationary structure of the upstream gas dynamic portion of the jet outflowing into a vacuum chamber in a wide range of p_0/p_∞ ratio ($20 \div 200$, 10^3, 10^8) with p_0 being stagnation pressure of the outflowing gas and p_∞ the ambient pressure, for the air, Ar, N_2 CO_2 and mixtures of N_2+CO_2+He at stagnation temperatures of up to 2500°K.

The wave structure of the nonstationary jet was investigated in the detail with the gas outflowing into the vacuum chamber with a counter-pressure of 30–40 mm. Hg, the gas being heated by a reflected shock wave in a shock tube. The process was recorded by means of the type IAB-451 schlieren instrument with a spark source [1, 5, 6].

The photographs shown in Fig. 1 (a, b, c) illustrate successive stages of changing the structure of the nonstationary flow of N_2, Ar and CO_2 when the gas outflows through a slit. The pictures 2, 3, 4 as well as 5 and 6 for CO_2 give a typical disturbance associated with the front of the outflowing gas.

The surface of the front of the outflowing gas (II in Fig. 1a) is a slip stream separating the vacuum chamber gas and the gas outflowing through the slit from the volume heated by the reflected shock wave in the shock tube. The surface has the same specific structure for Ar and N_2, and is somewhat different for CO_2, in which case, it is more complex and more disturbed at the initial stage. The subsequent photographs show it to become more stable and distinct later on, and then to diffuse considerably later than in the cases of Ar, N_2 and air.

The outflow of gas through a circular sound nozzle at the initial stage of the nonstationary condition does not differ from that through a slit. In the immediate vicinity of the nozzle exit there develop disturbances associated with the outflow front (Fig. 2) and forming a system of rings. In the present experimental conditions three rings were formed during the first 45–75 μsec. The second and third rings noticeably increase with time, while the size of the first ring remains constant and 100–125 μsec later its contours become indistinguishable in a turbulent structure resulting from the growth and disintegration of the second ring. During first 25 μsec the disturbance formed before the outflow front is a front of interference of the disturbances of each of the vortex rings, i.e., the envelope of the disturbed region is not smooth and repeats the structure of the system of rings. After 35–45 μsec the front of the disturbed region is at a sufficiently long distance from the contact surface, is smooth and of an approximately elliptic shape with the large axis parallel to the flow.

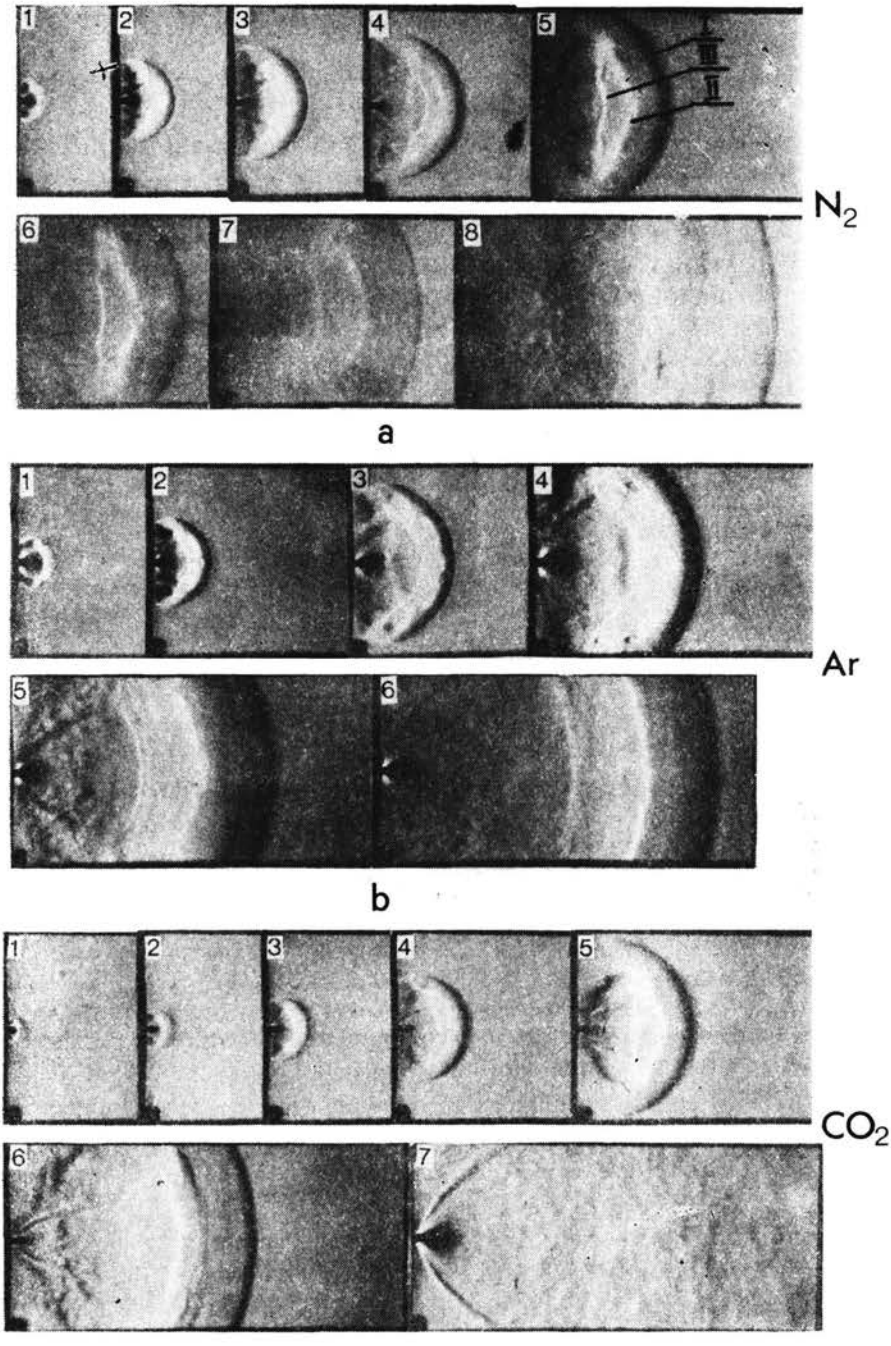

FIG. 1.

The data were quantitatively processed by writing down approximation formulas to describe the propagation of the disturbance front with time. The results are conveniently presented in non-dimensional coordinates. The distance in $X\left(X=\frac{x}{r_*}\right)$ where the disturbance is observed at a moment t, is shown as a function of non-dimensional time $T=\frac{tc_*}{r_*}$, where c_* is the critical sound velocity in the outflowing gas, r_* is the critical radius of a nozzle and x is the coordinate along the outflow. The time T shows how the moment of observation relates to the time required for the disturbance to cover a characteristic dimension of the flow at the critical sound velocity. The latter quantity entering the definition of T, carries information about the initial state of the outflow gas, as for the ideal gas it is a single-valued function of receiver temperature.

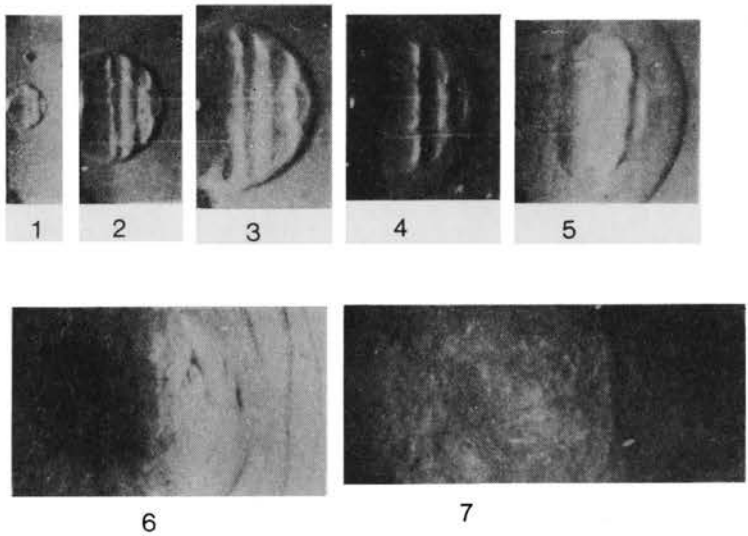

FIG. 2.

In the case of the shock-heated gas the gas parameters in the receiver are those behind the reflected shock wave. The equilibrium and completely frozen state behind the reflected shock waves in CO_2, for the conditions corresponding to the Mach number $M \leqslant 4$, have temperatures differing by 20–25%. In N_2 the difference is much less, while in Ar at $M \leqslant 4$ ionization gives no noticeable change in temperature behind the reflected shock wave.

When treating the experimental data, it is assumed that the state in CO_2 and N_2 behind the shock wave corresponds to the equilibrium excitation of the gas molecules. The critical sound velocity was calculated neglecting the relaxation effects.

These calculations are based on comparatively small effect of γ variation on the sound velocity under the given conditions (6–7%). In principle, the specific properties of the real gas when determining c_* would be of importance particularly under the gas outflow conditions due to the reflection of shock waves with $M \geqslant 4$ in above-mentioned gases.

In coordinates X, T, the experimental points for each gas lie on a single curve, the curves being different for each of the gases under investigation.

Table 1

Gas	Coefficients			
	Shock wave front		Outflowing gas front	
	A	α	A	α
CO_2	3.8	0.71	3.2	0.68
Ar	3.1	0.69	2.5	0.65
N_2	3.1	0.71	2.6	0.71

The experimental curves can be presented on the portion of the dependence of T on X as the T to the α-th power function:

$$\frac{x}{r_*} = A\left(\frac{tc_*}{r_*}\right)^{\alpha}, \tag{1}$$

where A and α are given in Table 1.

The agreement between the curves plotted from these formulas and the experimental points is illustrated by Fig. 3.

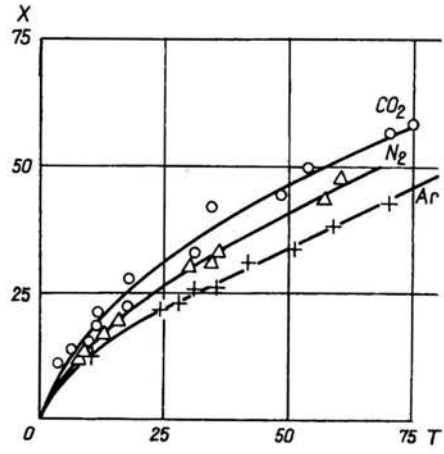

FIG. 3. The time dependence of the shock wave position along the flow axis for the slit.

From the approximation relations we may obtain formulas for the velocity

$$\frac{dx}{dt} = A\alpha\left(\frac{tc_*}{r_*}\right)^{\alpha-1} c_*. \tag{2}$$

The graphs of velocities for the case of outflow from the slit for the outflowing gas front are shown in Fig. 4. The velocity is related to the critical sound velocity $\left(V = \frac{dx}{dt}\frac{1}{c_*}\right)$.

The relations proposed are valid only in a region which is in agreement with the experimental points and cannot be applied to the final stage of the motion, since the conditions of transfer to the limit are not given in the relations of this kind. In the limit case the front of the compression wave propagationg in the vaccum chamber would move with the sound velocity until it is completly dissipated. The disturbance intensity may decrease differently, depending on the particular gas, but the compression wave velocity cannot be lower than that of sound in undisturbed medium. Therefore, the approximation curves for dx/dt are valid in the region $t \leqslant 75\,\mu$sec for N_2; $t \leqslant 100\,\mu$sec for CO_2 and $t \leqslant 175\,\mu$sec for Ar.

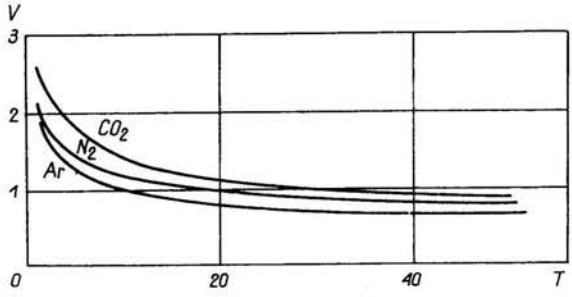

FIG. 4.

As shown by Figs. 1 and 2 initially ($t \leqslant 15\,\mu$sec) the disturbance front in the vacuum chamber and the boundary of the outflowing gas are indistinguishable. The disturbance front follows the form of the boundary of the outflowing gas, but becomes smooth and distinctly separates from it at 25–30 μsec.

Using the approximation relations and the time dependences of the non-dimensional velocity derived from there it has been found that for a period T in which the non-dimensional velocity exceeds 1.5, the wave front (and the outflowing gas front) move at a velocity exceeding that of the shock wave in the tube before its reflection from the tube end.

The time dependences of the shock wave position along the flow axis, as obtained from experiment, are shown in Fig. 5. The shock wave was propagated by the front of the gas outflowing from the circular sound nozzle.

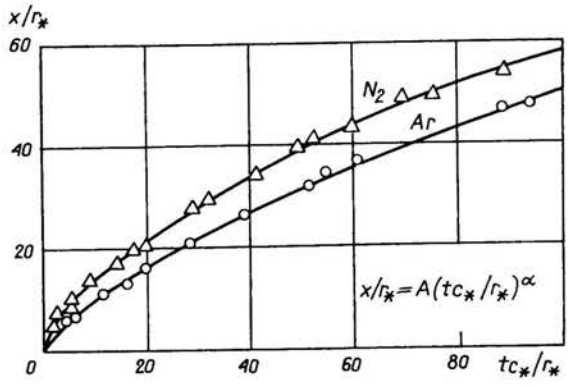

FIG. 5. The time dependence of the shock wave position along the flow axis for the circular sound nozzle.

The curves shown in this figure are described by approximate relations of type (1), where A and α are given in Table 2.

Table 2

Gas	Coefficient			
	Shock wave front		Outflowing gas front	
	A	α	A	α
N_2	3.04	0.66	3.00	0.54
Ar	2.72	0.63	2.62	0.52

The flow field was investigated by the method of absorption of an electron beam, with nonstationary outflow of Ar and N_2 from a circular sound nozzle having a diameter $d_* = 0.25$ mm, receiver pressure $p_0 \cong 7$ atm, at ambient pressure of $p_\infty = 2 \cdot 10^{-5}$ mm Hg room stagnation temperature of the outflowing gas and the ambient gas. As a result, the patterns of the gradient regions propagation at distances up to 600 d_* along the flow axis x and up to 350 d_* in the direction y normal to the axis have been determined [7].

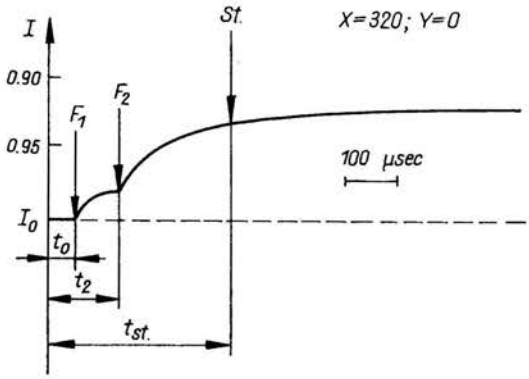

FIG. 6.

At an early stage, the front of the outflowing gas in a finite pressure volume is preceded by a shock wave. With the initial density of the external gas, under the present conditions being $\varrho_\infty = 3 \cdot 10^{-11}$ g/cm^3 the primary shock wave which did not increase the density more than by a factor of $4 \div 6$, could not increase the density above the sensitivity threshold. Therefore, all recorded absorption signals correspond to the increased density of the outflowing gas. The time interval F_1 on the oscillogram (see Fig. 6) is identified with the arrival of the outflow front to the point being investigated.

The time dependences of the shock wave position along the flow axis, as obtained from experiment, are shown in Fig. 7. The non-dimensional coordinates $T = \frac{tc_*}{r_*}$ and $X = \frac{x}{r_*}$ are plotted on the axes.

The empirical approximations of the equations of the outflow front propagation are determined by the least squares method, taking into account the time dispersion depend-

ence T on X coordinate. The dispersion has been found to change with an increase in X in proportion to X^2. This can be accounted for by an enhanced scatter of the experimental data, due to the decreased sensitivity of the method as the density lowers with distance from the nozzle exit, as well as by enhanced irregularities in the flow clearly distinguishable, e.g. in schlieren pictures in papers [1, 5].

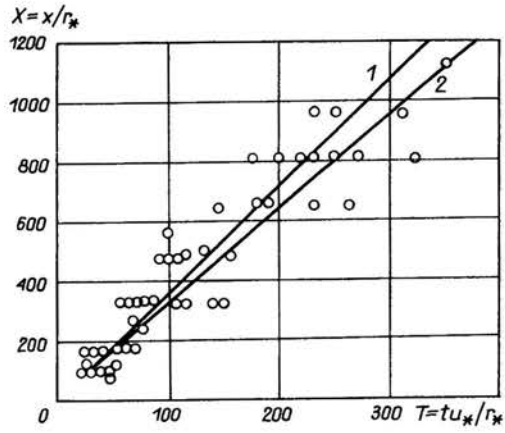

FIG. 7.

For the form of the equation of motion with an arbitrary exponent used in paper [5] it has been found that

$$T = 6.6+0.18\,X^{1.06} \tag{3}$$

and this corresponds to curve *1* in Fig. 7.

For the weighed regression in the form of a square trinomial it has been found (curve *2*, Fig. 7) that

$$T = 6.6+0.25\,X+6.6\cdot 10^{-5}\,X^2. \tag{4}$$

The free term in Eqs. (3) and (4) appears to be due to the delay in the outflow, and will be omitted further on.

The variation pattern of the velocity of the outflowing gas front is determined on the basis of equation of motion (4). At a distance x of 80 to 1200 r_* along the axis it is found to change from 1100 to 800 m/sec.

The analysis of the data obtained at the periphery points made it possible to draw a general picture of the space propagation of the front. Fig. 8a presents the curves of the position of the outflow front in terms of X and Y where $Y = \frac{y}{r_*}$ at different times, plotted over the averaged experimental data. As shown in the figure, the departure from the spherical symmetry of the flow is observed at a very early time ($T \sim 30, X \sim 200$).

Later, an axial symmetry of the flow, rather than a spherical one, becomes more pronounced and the outflow front less distinct.

It should be noted, however, that the curves in Fig. 8 characterize the propagation of gas with a density, which is not below sensitivity threshold, which does not exclude penetration of a less dense gas into the periphery regions.

The propagation of the second absorption rise and of the moment of reaching the stationary flow is found to be of a less regular nature.

Consequently, no analytical treatment was performed of the propogation of these flow regions, and consideration was confined to qualitative analysis.

Fig. 8b illustrates propagation of the second absorption rise. It is seen that in this case the spherical symmetry is violated from the very early stages of the process. Furthermore, the curves of Fig. 8 cannot be regarded as equal-density curves, because they correspond to different levels of integral absorption, i.e., they characterize the integral density along the way of the beam.

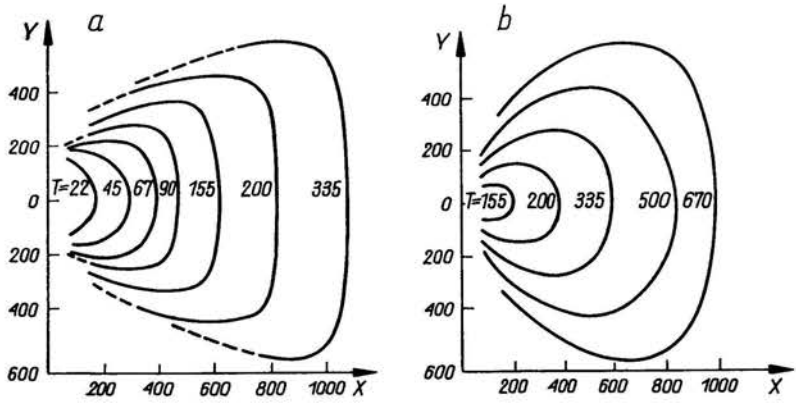

FIG. 8.

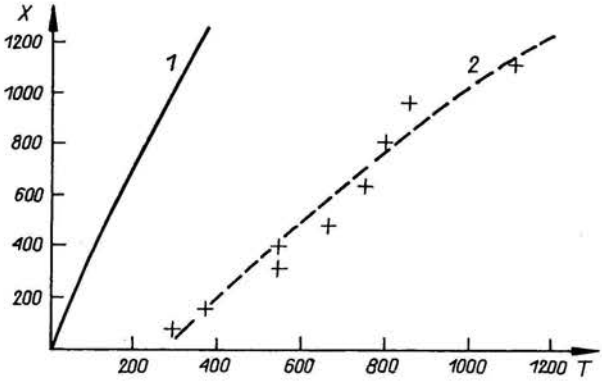

FIG. 9.

Fig. 9 presents an experimental time dependence of the propagation of the moment of establishing the stationary absorption along the outflow axis (curve 2). The asterisks show the values averaged over the data of 6÷8 experiments. Curve *1* in Fig. 9 is the motion of the outflow front.

In order to generalize the results obtained and to compare them with the data available for other regimes, as well as with calculation it was necessary to make use of the parameters, not only taking into account the specific nozzle dimension, but also accounting

for gas expansion in the flow. Such parameters suitable for describing the initial stage of the flow from a source are proposed in paper [4].

Fig. 10 presents the motion of the outflow front in terms of ζ and τ:

$$\zeta = \frac{x}{r_*}\sqrt{\frac{\varrho_\infty}{\varrho_*}}, \tag{5}$$

$$\tau = \frac{t}{t_*}\sqrt{\frac{\varrho_\infty}{\varrho_*}}, \tag{6}$$

where $t_* = \dfrac{r_*}{u_{\max}}$, $u = \dfrac{2}{\gamma-1}a_T$, ϱ_* is the critical density and a_T is the sound velocity at stagnation conditions. Curves *1* and *2* correspond to Eqs. (3) and (4) which may be written in coordinates ζ and τ as

$$\tau = 0.86\,\zeta^{1.06} \quad \text{(curve 1)} \tag{7}$$

$$\tau = 0.86\,\zeta + 5.1\,\zeta^2 \quad \text{(curve 2)}. \tag{8}$$

The horizontal dashed line represents the maximum value of ζ in the present experiments. Curve *3* is the motion of the outflow front in the experiments of paper [5]:

$$\tau = 1.4\,\zeta^{1.92}. \tag{9}$$

The difference in the range of ζ and τ variation illustrates the difference of the physical conditions of expansion in the present experiments.

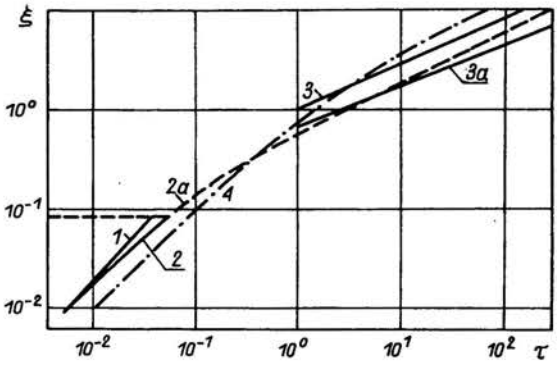

FIG. 10.

The hatch-dash line *4* is the calculation equation of the front motion obtained on the basis of paper [4].

$$\tau = \zeta + 0.46\,\zeta^2. \tag{10}$$

The asymptotic form of this equation of motion, considered in [4] shows that the square term becomes important with sufficient counter-pressure by the ambient gas. At an early stage of the expansion, or when the gas outflows into a vacuum, the front motion is shown approximately to be described by a linear law. This has been confirmed by the present experimental data. Thus, comparison of Eqs. (9) and (7) indicates an approximately

square-law relation ($\tau \sim \zeta^{1.92}$) at $\zeta \geqslant 1$ and its approach to a linear form ($\tau \sim \zeta^{1.06}$) at $\zeta < 10^{-1}$.

For the equation of motion in the form of a quadratic binomial (8) it can be seen that the linear term exceeds the quadratic term in the whole range of the present experimental data. Extrapolation of this equation of the front motion to large parameters shows fair coincidence of the effective exponents in Eqs. (8) and (9) at $\zeta > 1$, which is an evidence of the important role, of the counter-pressure at this stage of the process.

The low experimental value of the velocity at $\zeta > 1$, as compared to the calculation for the source, may be associated with the energy losses for vortex motion clearly seen on all schlieren pictures taken at a higher pressure in the receiver (Fig. 2). But in the experiments with low pressure ($\zeta < 10^{-1}$) the vortex motion might be a cause of the large scatter in the experimental data.

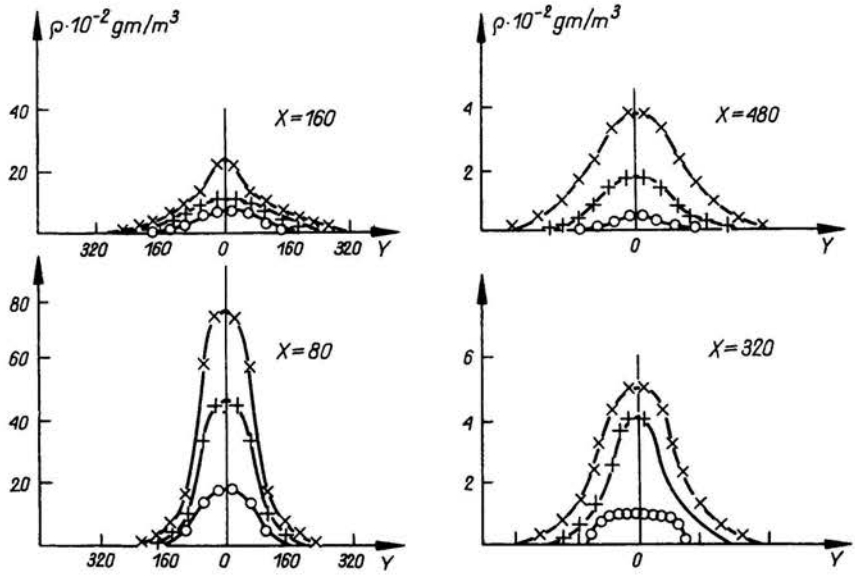

FIG. 11.

If the results on the front propagation are generalized taking account of the temperature factor, the experimental values for shock-heated gas are found to be in good agreement with extrapolated dependence (8) for $T = 300°K$ (curve *3a* and dote-curve *2a* in Fig. 10).

Still another region of a sudden change in the density characteristic of the non-stationary outflow is the secondary shock wave. When the jet is formed in a volume with a comparatively high counter-pressure, a secondary shock wave is formed and observed in the vicinity of the nozzle exit, whereas at small values of p_∞ no secondary shock wave has been observed.

Also worth noting is the information concerning the density and its variation with time and distance for specific conditions of the non-stationary outflow of Ar shown in Fig. 11. However, it is clear that the complex structure of the flow would require local

measurements. The data obtained in the present study by calculation, based on the measurements of the total absorption, can give only preliminary information concerning the general tendency in the gas outflow close to the nozzle exit in the process of jet formation.

The present investigation has shown that the initial stages of the supersonic outflow into vacuum chamber with a counter-pressure have a specific wave structure, close to the front motion of the outflowing substance.

The non-stationary wave structure of the gas-dynamic portion of the jet is specific for different gases.

It has been found that none of the elements of the wave non-stationary structure associated with the front motion of the gas becomes an elements of the stationary jet structure.

In order to generalize the results obtained to the case of motion of the front of the outflowing substance along the flow, and to compare them with calculation of the models of the flow from a spherical source available in literature, the data are given in coordinates carrying the information on the flow boundary conditions.

It has been found that time of formation of a stationary geometric structure of the gas-dynamic portion of the jet is approximately by an order of magnitude higher than those which could be obtained from literature data.

Density distribution in non-stationary rarefied Ar and N_2 jets has been plotted throughout the flow field for the non-stationary stages of process.

References

1. I. M. Naboko, T. V. Bazhenova, A. I. Opara, V. A. Belavin, *Formation of a jet of shock-heated gas outflowing into a evacuated space*, Astr. Acta, **17**, 653–658, 1972.
2. В. Н. Гусев, *К вопросу о запуске сверхзвуковых сопел*, Инж. Журнал, **1**, 1, 1961.
3. G. A. Simons, *The large time behaviour of a steady spherical source expanding into an arbitrary ambient gas*, AIAA Paper, 70, p. 232, 1970.
4. С. Ф. Черкмарев, *Неустановившееся радиальное расширение газа в затопленное пространство от внезапно включенного стационарного источника*, Журнал Прикл. Мех. и Техн. Физ., **2**, 70–80, 1975.
5. В. А. Белавин, В. В. Голуб, И. М. Набоко, А. И. Опара, *Исследование нестационарной структуры потока при истечении ударно-нагретого газа*, Журнал Прикл. Мех. и Техн. Физ., **5**, 1973.
6. И. М. Набоко, Е. М. Кудрявцев, А. И. Опара, В. Р. Голуб, *Структура потока ударно-нагретого газа в условиях импульсного газодинамического лазера*, Теплофиз. Высоких Темп., **12**, 1, 122–128, 1974.
7. А. В. Еремин, В. А. Кочнев, И. М. Набоко, *Исследование формирования струи газа при истечении в разреженное пространство*, Журнал Прикл. Мех. и Техн. Физ., **2**, 1975.

INSTITUTE FOR HIGH TEMPERATURES,
MOSCOW, USSR.

Received April 29, 1976.